

Identification of subsurface structure using the pseudo-gravity method of magnetic data at the geothermal area of Sonai Village and its surroundings, Puriala, Konawe Regency

Misbayanti Dian Ratu¹, Abdul Manan^{1*}, Bahdad², and Rani Chahyani³

¹Department of Geophysical Engineering, Universitas Halu Oleo, Kendari 93232, Indonesia

²Department of Oceanography, Universitas Halu Oleo, Kendari 93232, Indonesia

³Study Program of Physics Education, Institut Agama Islam Negeri Kendari, Kendari 93116, Indonesia

*Corresponding author: amanan@uho.ac.id

ABSTRACT

It has been conducted a geomagnetic research in the geothermal area of Sonai Village and its surroundings, Puriala, Konawe Regency, which aims to identify the structure of the subsurface using the pseudo-gravity method. After performing diurnal and IGRF corrections on the measurement data, the residual magnetic field anomaly is obtained around -150 to 90 nT. Furthermore, transformation process using the pseudo-gravity method is carried out, and the anomaly contour density is obtained around -0.07 to 0.06 mGal. The results of 2D modeling of 2 slices on the residual magnetic anomaly map that have undergone pseudo-gravity transformation show that the subsurface layers of the research area are composed of 3 formations. Layers with density values of 1.5 and 2.5 g/cm³ are thought to be Alluvium Deposits in the form of sand and clay, layers with density values of 2.6 and 2.78 g/cm³ are sandstone and conglomerate in the Alangga Formation, and a layer with a density value of 2.84 g/cm³ is peridotite in the Ultramafic Complex (bedrock layer). In addition, several minor faults were also found, and among them 2 minor faults adjacent to geothermal manifestation are located at coordinates of approximately 4°1'16.149" South Latitude dan 122°7'9.609" East Longitude with a distance of ±15 meters, and at coordinates of approximately 4°1'23.388" South Latitude dan 122°7'24.326" East Longitude which is ±28 meters from the manifestation. These minor faults cut through the peridotite layer and the conglomerate layer, and are thought to be the migration path of hot fluids towards the surface.

Keywords: Geothermal area; magnetic anomaly; pseudo-gravity method; subsurface structure

Received 01-06-2025 | Revised 30-06-2025 | Accepted 08-07-2025 | Published 31-07-2025

INTRODUCTION

Sulawesi Island is one of the islands where most of the geothermal potential is associated with a non-volcanic geological environment. The Sulawesi region in the southeast has the geothermal potential spread from mainland Sulawesi to Buton Island. The geothermal system on the mainland is more influenced by the combination of the influence of geological structure and the remaining heat from magmatic activity, generally appearing in the metamorphic and sedimentary rock environment [1, 2]. The non-volcanic geothermal system is usually associated with the existence of faults in the subsurface of the Earth [3-5]. One area in the Southeast Sulawesi

that has the geothermal potential is in Sonai Village, Puriala District, Konawe Regency.

Geothermal system is a natural heat transfer in a certain volume of the Earth's crust that carries heat from the heat source to the place of heat release, which is generally the ground surface. Generally, rocks in geothermal systems have low magnetization due to the demagnetization process by the hydrothermal alteration process. This process changes existing minerals into paramagnetic and diamagnetic minerals [4, 5].

The Sonai geothermal area was studied by the Geological Agency of the Ministry of Energy and Mineral Resources RI in 2015 in the form of a preliminary geochemical survey [6]. Then [7] also studied this area to determine

the distribution of hot fluids using the Wenner-Schlumberger configuration geoelectric method. The latest, [8] studied this geothermal area using the Euler Deconvolution method.

In this research, the magnetic method was used to determine the types of rock layers and the possibility of faults existence in the Earth's subsurface. The geomagnetic method works based on the magnetic properties of subsurface rocks which are known through measurements of the intensity of the magnetic field on the Earth's surface [9, 10]. To clarify the location of the object causing the subsurface anomaly, a transformation using the pseudo-gravity method was carried out on residual magnetic field anomaly data.

Geophysical researches on geothermal using geomagnetic method, some of which have been conducted by [11] at Buaran geothermal manifestation area Brebes Regency, [12] at geothermal area of Umbul-Telomoyo Temple Magelang Regency, [13] at geothermal manifestation of Karangrejo Pacitan Regency, [14] at the Banyu Biru hot spring Nganjuk Regency, [15] at Sampuraga geothermal manifestation area Mandailing Natal Regency, [16] at Nagari Aie Angek geothermal prospect area Tanah Datar Regency, and [17] at the Tinggi Raja geothermal area Simalungun Regency. The results of these studies show that the magnetic method provides good results in identifying the subsurface structure of geothermal potential area.

LITERATURE REVIEW

Regional Geology of Research Area

Regionally, Puriala District is included in the geological map of the Kolaka Sheet [18]. Based on the rock assemblage and its characteristics, the geology of the Kolaka Sheet can be divided into two geological belts, namely the Tinodo Belt and the Hialu Belt. The rocks found in the Tinodo Belt which are the basement rocks are Paleozoic Metamorphic Rocks (Pzm) and are thought to be of Carboniferous age, consisting of mica schist,

quartz schist, chlorite schist, graphite mica schist, slate and gneiss. Meanwhile, the rocks found in the Hialu Belt are Ophiolite Rocks (Ku) consisting of peridotite, harzburgite, dunite and serpentinite. These Ophiolite rocks are unconformably overlain by the Matano Formation (Km) of Late Cretaceous age and consist of layered limestone intercalated with chert at the bottom. Molasse type sedimentary rocks of Late Miocene-Early Pliocene age form the Pandua Formation (Tmpp) consisting of conglomerate and sandstone intercalated with silt. This formation unconformably overlaps all older formations, both in the Tinodo Belt and the Hialu Belt. In the Late Pleistocene, coral reef limestone (Ql) and the Alangga Formation (Qpa) were formed, consisting of sandstone and conglomerate. The youngest rocks in this sheet are Alluvium (Qa) consisting of river, swamp and beach deposits [19, 20].

The Sonai area which is the research location is included in the Hialu Belt which consists of Alluvium Deposits, the Alangga Formation and the Ultramafic Complex. The distribution of the geological conditions of the research location is shown in Figure 1.

Magnetic Method

The magnetic method is one of the geophysical methods interpreted in the form of magnetic material distribution based on the measurement of variations in magnetic field intensity on the earth's surface. This method is carried out based on the results of magnetic field intensity measurements caused by differences in susceptibility contrast or magnetic permeability of rocks from the surrounding area [10, 21].

The basis of the magnetic method is the Coulomb force F (dyne). If there are two magnetic poles P_1 and P_2 that are separated by a distance of r (cm), then there will be a Coulomb force F of [10]:

$$\vec{F} = \frac{P_1 P_2}{\mu_o r^2} \hat{r} \quad (1)$$

where, μ_0 is the permeability of the medium in a vacuum, is dimensionless and has a value of 1, and r represents a unit vector in the direction from P_1 to P_2 . The value of μ_0 in SI units is $4\pi \times 10^{-7} \text{ N/A}^2$.

Pseudo-Gravity Method

[22] explained that the pseudo-gravity method is a transformation that makes the magnetic anomaly value comparable to the gravity anomaly value. Pseudo-gravity transformation is one method that functions to clarify the location of objects causing subsurface anomalies [23]. The working principle of the pseudo-gravity method uses the Poisson relation. This relation states that the

magnetic potential V and the gravitational potential U originating from a uniform density or a uniformly magnetized object have a relationship like the formula below [22]:

$$V = \frac{C_m}{\gamma} \frac{M}{\rho} m \cdot \nabla_p U = -\frac{C_m}{\gamma} \frac{M}{\rho} g_m \quad (2)$$

where, V is the magnetic potential, U the gravitational potential (m/s^2), m the direction of magnetization, g_m the component of the gravitational force in the direction of magnetization, γ Newton's constant ($6.67 \times 10^{-11} \text{ m}^3\text{kg}^{-1}\text{sec}^{-2}$), ρ the density of the rock (kg/m^3), C_m the magnetic constant, and M the magnetization (A/m).

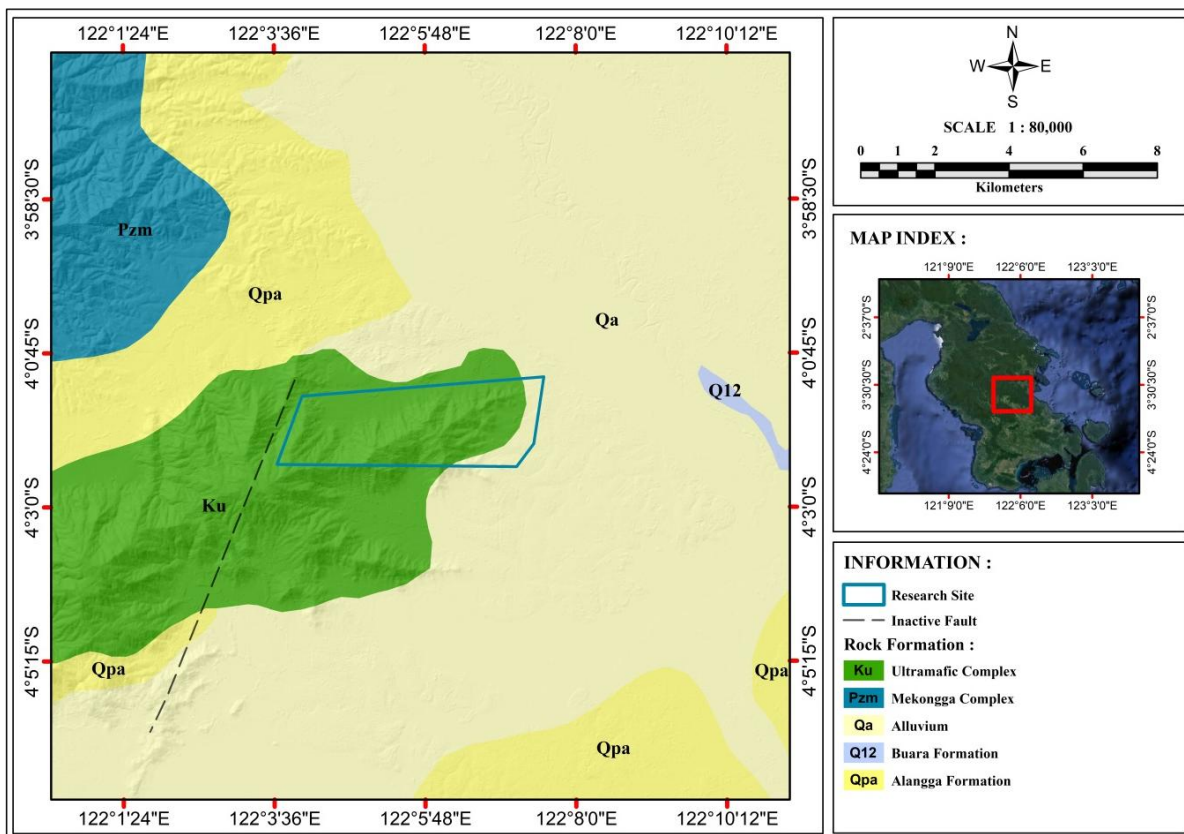


Figure 1. Regional geological distribution for the research area [8].

RESEARCH METHODS

Research Location and Data

This research uses measurement data from 1 set of Proton Magnetometer and Gradiometer

PMG-2 instruments carried out on November 12 – 13, 2023 at Sonai Village and its surroundings, Puriala District, Konawe Regency, Southeast Sulawesi Province. Measurements were carried out at 126 points in

6 trajectories in the N180°S direction. The location of the measurement points can be seen in Figure 2. In addition, this research also uses secondary data in the form of magnetic

inclination and declination angles of the research area sourced from the International Association of Geomagnetism and Aeronomy (IAGA) website.

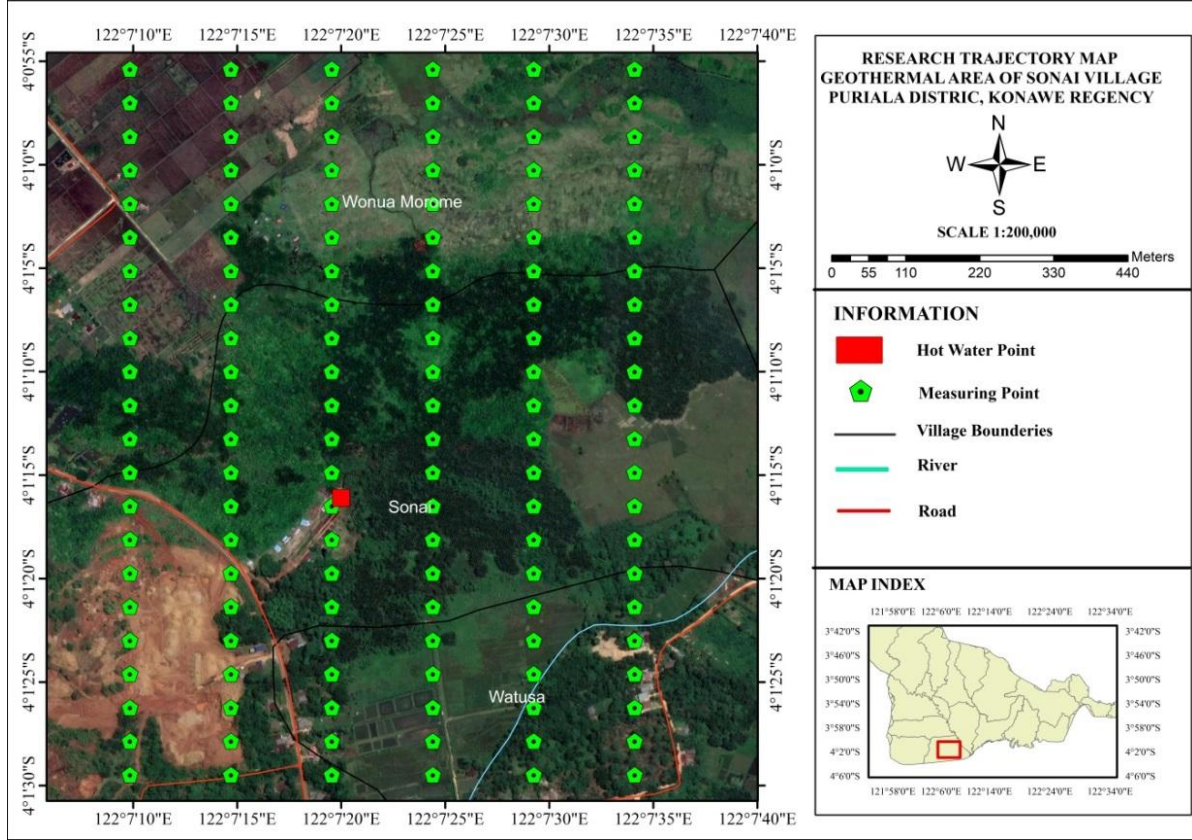


Figure 2. Distribution of measurement points.

Data Processing

Diurnal Correction

Diurnal Correction is a correction made to magnetic field data measured in the field to eliminate the influence of external magnetic fields or daily variations. The calculation of diurnal correction is done using Microsoft Excel 2016 with the formula [24, 25]:

$$\Delta H_{daily} = \left(\frac{t_n - t_{in}}{t_e - t_{in}} \right) (H_e - H_{in}) \quad (3)$$

where, ΔH_{daily} is the diurnal correction, H_e is the magnetic field value at the end point, H_{in} is the magnetic field value at the starting point, t_{in} is the measurement time at the starting point, t_e is

the measurement time at the end point, and t_n is the measurement at point n.

IGRF Correction

IGRF correction is a correction performed to measured magnetic field data that has undergone diurnal correction to eliminate the influence of the Earth's main magnetic field. IGRF values is obtained from the website of The International Association of Geomagnetism and Aeronomy (IAGA). IGRF correction is calculated using the equation [24, 25]:

$$\Delta H_t = H_{daily} \pm \Delta H_{daily} - H_o \quad (4)$$

where, ΔH_t is the total magnetic field anomaly, H_{daily} is the H value at each measurement point, ΔH_{daily} is the diurnal correction, and H_o is

the IGRF correction of the Sonai Village geothermal area and its surroundings.

Upward Continuation Transformation

Upward Continuation transformation is the process of transforming potential field data from a flat plane to a higher flat plane. In magnetic method data processing, this process functions to reduce residual magnetic effects originating from various sources of magnetic objects spreaded on the topographic surface that are not related to the survey [26, 27]. The result is a regional magnetic field anomaly (ΔH_{upward}).

Obtaining Residual Magnetic Field Anomaly

The regional magnetic anomaly that have been obtained is further processed to obtain residual (local) magnetic anomaly that are the target of the research. The anomaly is obtained following the equation [8, 24, 25]:

$$\Delta H_{\text{res}} = H_t - \Delta H_{\text{upward}} \quad (5)$$

where, ΔH_{res} is the residual magnetic anomaly, ΔH_t is the total magnetic anomaly and ΔH_{upward} is the regional magnetic anomaly resulting from Upward Continuation transformation.

Application of Pseudo-Gravity Method

The pseudo-gravity method is carried out to eliminate the polarity effects of the magnetic method by converting magnetic anomaly data as if it were a gravity anomaly or pseudo-gravity. This transformation process follows equation (2). The density contrast value according to [26] is 0.1 gr/cm₃ per A/m where 1 A/m is 0.001 Gauss.

Performing 2D Modeling

2D modeling is generated from slices made on the residual magnetic anomaly map that has undergone pseudo-gravity transformation. The goal is to obtain a 2D cross-section of the layers

and subsurface geological structures of the Sonai Village geothermal area and its surroundings.

RESULTS AND DISCUSSION

Total Magnetic Field Measurement Results

Based on the results of magnetic field measurements measured directly in the field using 1 set of Magnetometer and Gradiometer PMG-2 instruments, it is known that the total magnetic field value of the geothermal area of Sonai Village and its surroundings ranges from 42,220.59 nT to 42,469.21 nT. Figure 3 shows the contour of the total magnetic field anomaly that has not been corrected with Diurnal and IGRF corrections on the topography.

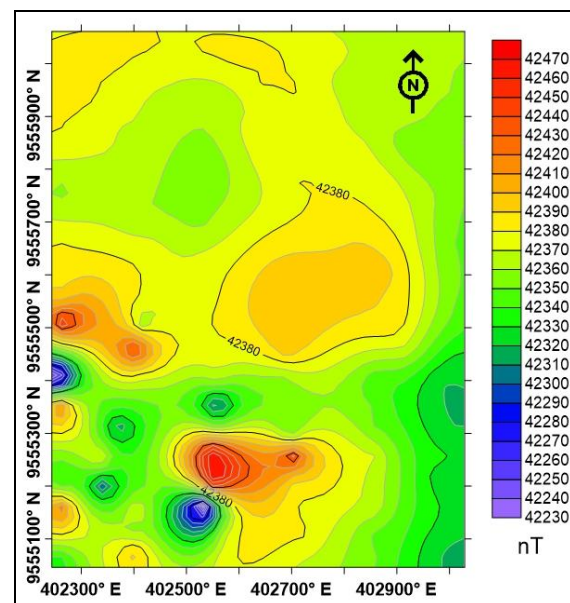


Figure 3. Uncorrected total magnetic field contour of the measurement results.

Corrected Total Magnetic Field Anomaly

The total magnetic field anomaly value that has undergone diurnal and IGRF corrections in the research area is around -171.17 nT to 82.47 nT. In general, the distribution of the total magnetic field anomaly pattern in the research area has three different anomaly trends which can be seen in Figure 4. The distribution of the high anomaly pattern with an anomaly range of around 10 nT to 82 nT is dominant in the North

with a lineage direction from West to Northeast. This high anomaly pattern decreases towards the West. The moderate anomaly pattern with an anomaly value range of around -90 nT to 10 nT is dominant in the South of the research area. This moderate anomaly has a decreasing trend from North-Northwest to West-Northwest. While the low anomaly pattern of around -171 nT to -90 nT is dominant in the South and Southwest of the research area.

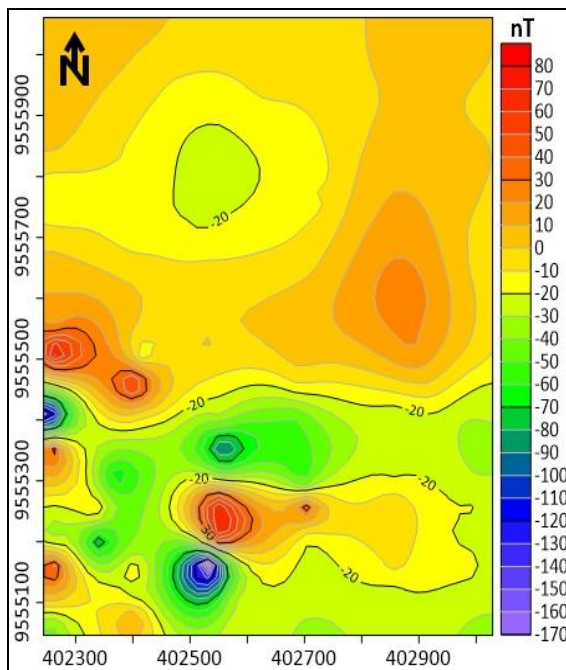


Figure 4. Corrected total magnetic field anomaly contour.

Performing Upward Continuation

Upward Continuation transformation of total magnetic field anomaly data was performed at heights of 100 m, 150 m, 200 m and 250 m as shown in Figure 5. This was done to see whether there were differences in the regional anomaly contour patterns of the research area at each specified height. In this research, the Upward Continuation process was stopped at a height of 250 m because the pattern on the contour map had shown a fairly smooth pattern and no longer experienced significant changes in closure. This shows that the pattern at this height can be considered to have experienced a separation between regional anomalies from the total magnetic field anomaly.

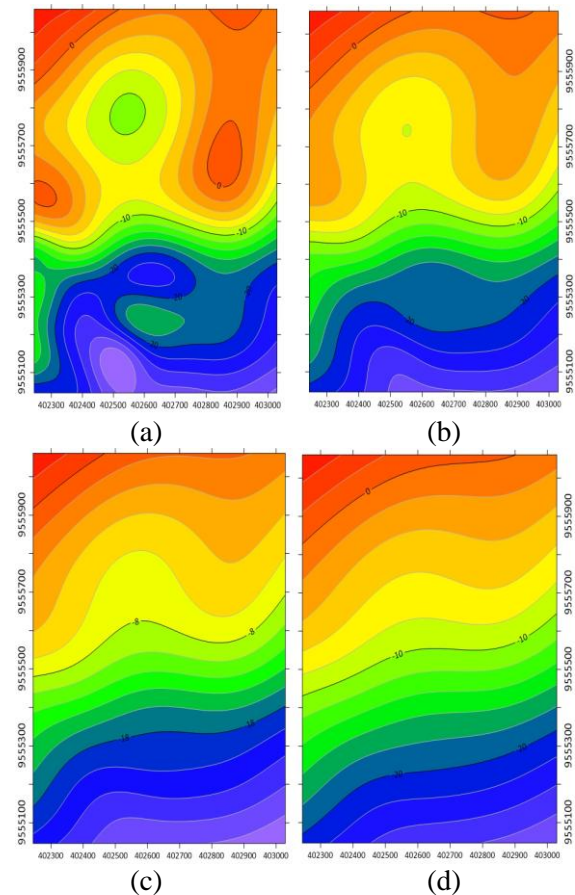


Figure 5. Contours of Upward Continuation at heights of (a). 100 meters, (b). 150 meters, (c). 200 m, and (d). 250 m.

Distribution of Residual Magnetic Field Anomaly

Separating the anomaly with Upward Continuation produces a regional anomaly map, so to get the residual anomaly it is done by subtracting the total magnetic field anomaly map and the resulting map from Upward Continuation. The residual magnetic anomaly contour map depicts the regional geological structure pattern in the research area.

The contours in Figure 6 show qualitatively areas with high and low susceptibility. The residual magnetic anomaly value contour obtained ranges from around -150 nT to 90 nT where moderate to high anomalies are dominant in the Northern part of the research area and low anomaly contours are dominant in the Southern part.

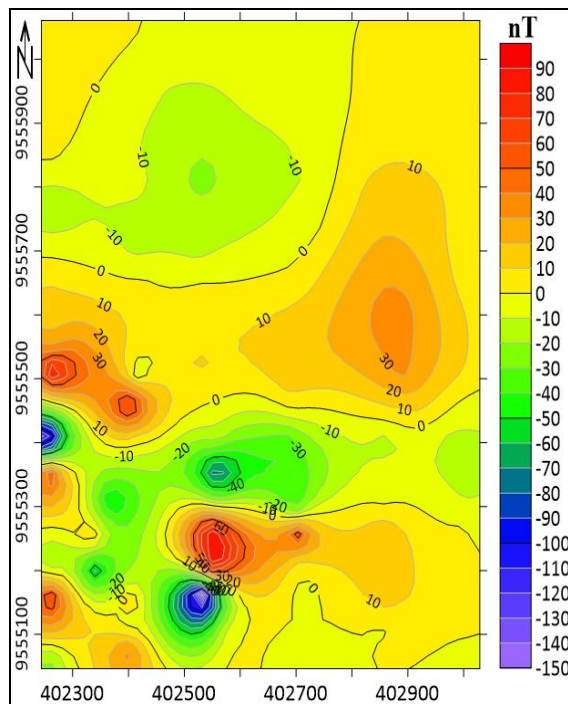


Figure 6. Contour of residual magnetic field anomaly.

Application of Pseudo-Gravity Method on Residual Magnetic Field Anomaly Data

The results of the pseudo-gravity method applied to the residual anomaly data have clarified the location of the subsurface anomaly target by displaying a simpler and more informative pseudo-gravity anomaly contour with a contour density of around -0.07 mGal to 0.06 mGal which can be seen in Figure 7 (a). This figure shows that the positive anomaly contour closure dominates in the North to the South of the research area. This positive anomaly is thought to be caused by rocks that have a relatively high density, so that in this section it is estimated to be dominated by ultrabasic rocks which in this case are peridotite rocks. While the West is dominated by negative anomalies which are interpreted to be composed of Alluvium Deposits.

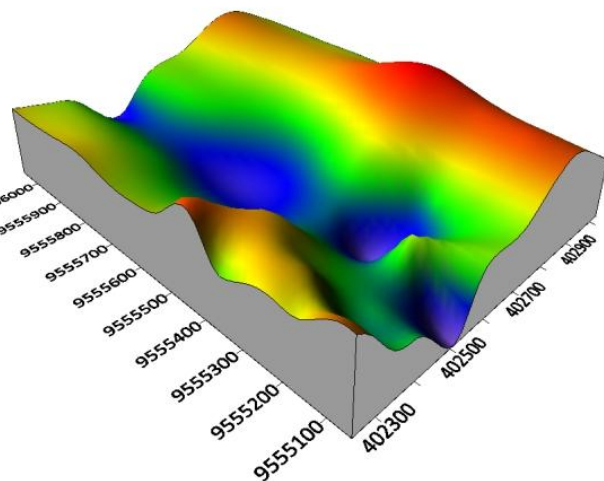
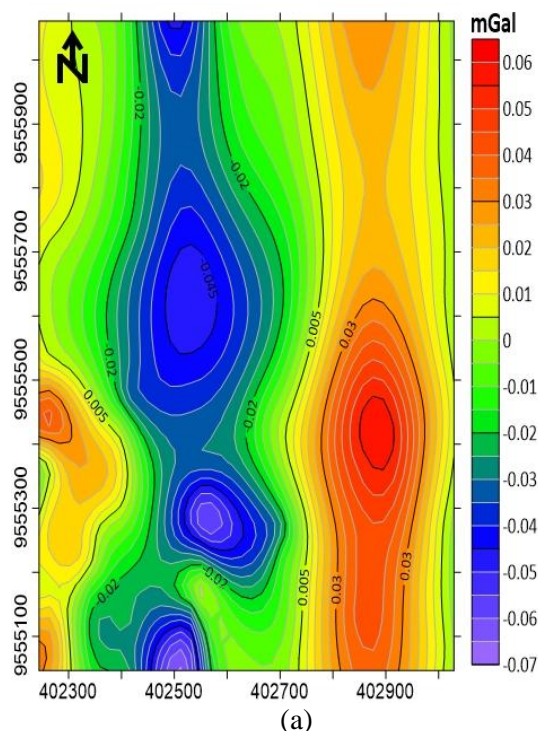


Figure 7. (a) Pseudo-gravity anomaly contour and (b) 3D map of pseudo-gravity anomaly.

In the research area, there is a fluid basin marked by the presence of different height distributions as can be seen in 3D in Figure 7 (b). The dense contour indicates a relatively high-density area, marked with green to red colors which are interpreted as contour patterns

that characterize the height that limits the fluid basin. While the loose contour indicates a relatively low-density area, marked with purple to blue colors which are a fluid basin.

The existence of geological structures in the form of faults in the research area can be

estimated from Figure 7 (a). This is based on the characteristics of the existence of fault in the form of anomalous lineation, contour density, anomalous deflection and anomalous polarization (negative and positive). Therefore, the White Box in Figure 8 is the estimated location of the existence of faults in the research area.

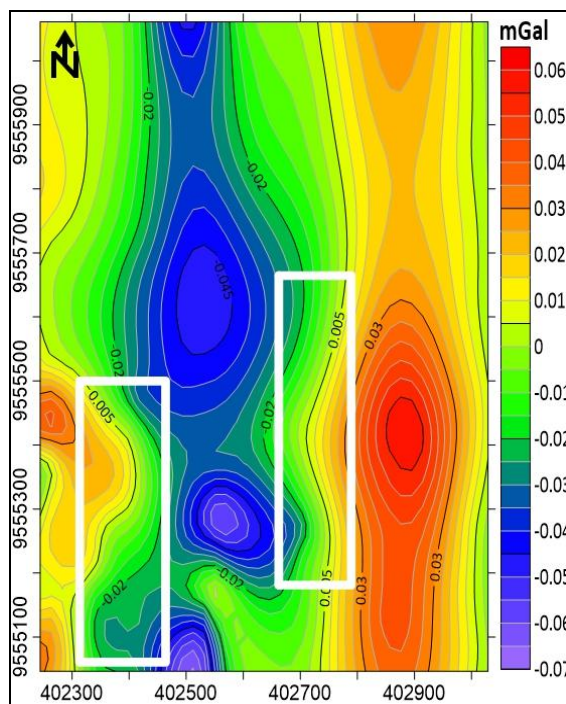


Figure 8. Estimated presence of faults on the pseudo-gravity anomaly map.

Creating Slices on Pseudo-Gravity Map

In this research, the number of slices modeled in an effort to know the existence of subsurface structures is 2 slices which are considered to have represented the research area. The drawing of slices is carried out from West to East or slice A-A' and from East-Southeast to Northwest or slice B-B', and the drawing of these slices can be seen in Figure 9.

2D Modeling and Geothermal Resources

The 2D modeling performed based on the results of the slices in Figure 9 is shown in Figure 10 and Figure 11 respectively. Interpretation of the 2D model was performed at an error value of <10%. The slices on the

pseudo-gravity anomaly map will produce an observation graph that can be used as a reference to estimate the layer structure and the presence of geological contacts in the subsurface. Based on the results of 2D modeling, the results for the A-A' and B-B' slices generally pass through 3 formations, namely Alluvium Deposits, Alangga Formation and Ultramafic Complex.

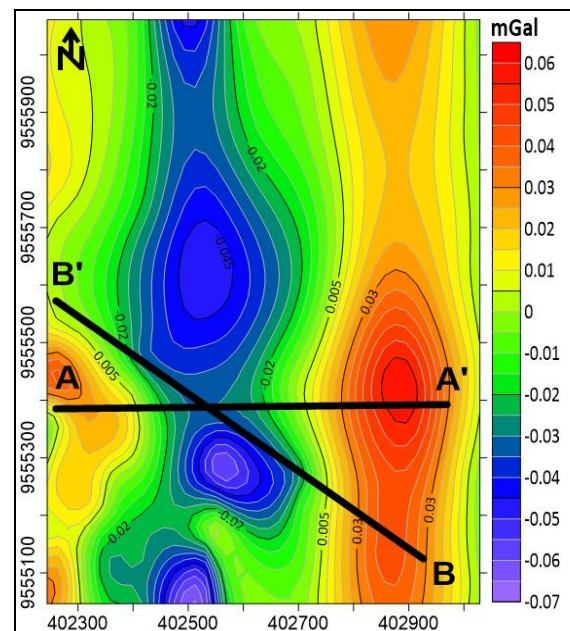


Figure 9. Direction of slices A-A' and B-B'.

2D modeling of the A-A' section in Figure 10 shows the presence of 3 layers. The first layer is composed of material with a density value of 1.5 g/cm^3 which is thought to be sand and a density of 2.5 g/cm^3 which is thought to be claystone. The material in the first layer is part of the Alluvium Deposit in the form of swamp and river deposits located near the manifestation (hot springs). In the second layer, a density value of 2.78 g/cm^3 is thought to be conglomerate rock and a density value of 2.6 g/cm^3 which is thought to be sandstone, and both are part of the Alangga Formation. In the third layer, there is an Ultramafic Complex with a density value of 2.84 g/cm^3 which is thought to be peridotite rock.

For Figure 11 which is the result of 2D modeling for the B-B' slice, 3 layers were also obtained. For the first layer, there is rock with a density value of 2.32 g/cm^3 which is thought to

be sandstone and is a part of the Alangga Formation, rock with a density value of 2.5 g/cm^3 which is thought to be Alluvium Deposits in the form of claystone, and rock with a density value of 1.5 g/cm^3 which is thought to be sand. In the second layer, there are rocks with a density value of 2.78 g/cm^3 which is

thought to be conglomerate, dominant in the East-Southeast part of the research area, while in the Northwest part there is sandstone. In the third layer, there is rock with a density value of 2.84 g/cm^3 which is thought to be peridotite from the Ultramafic Complex.

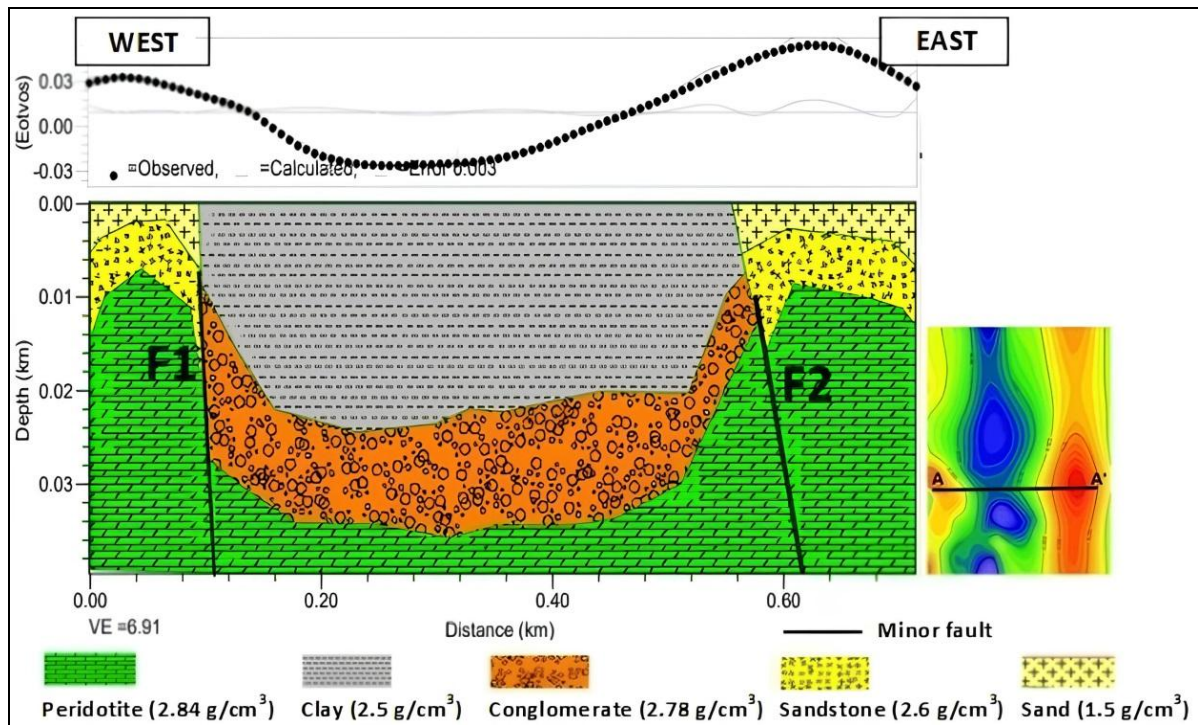


Figure 10. 2D modeling results for slice A-A'.

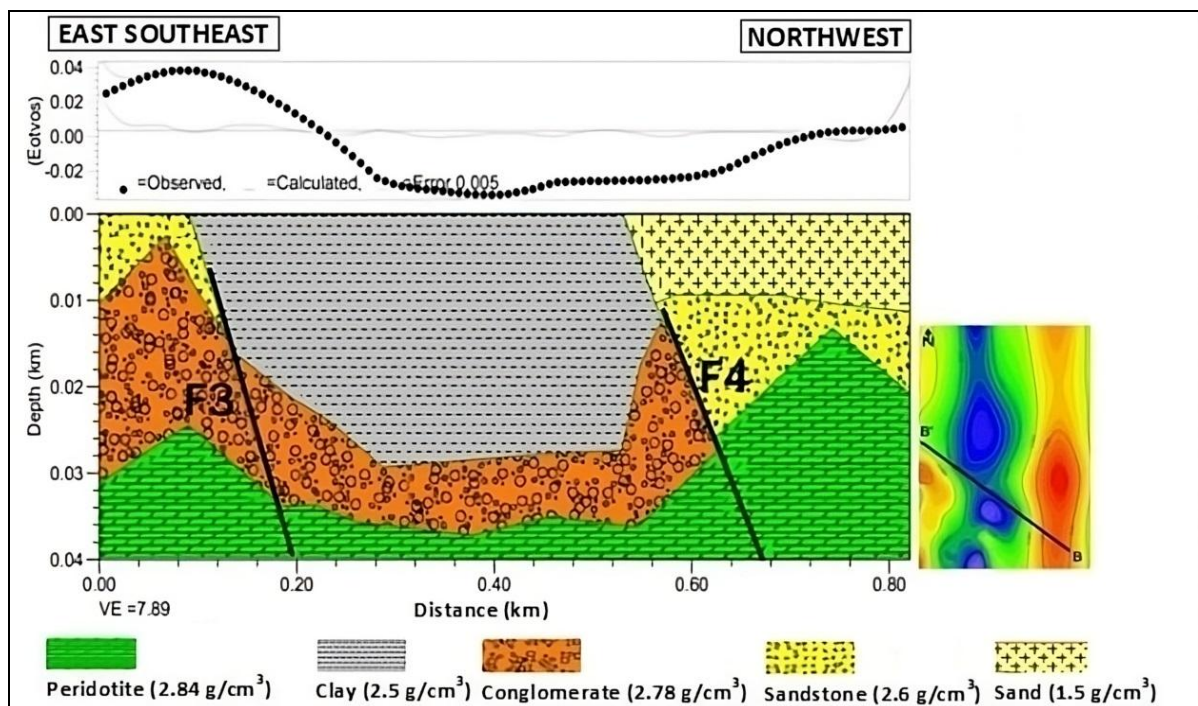


Figure 11. 2D modeling results for slice B-B'.

The results of the research in Figure 10 and Figure 11 are in accordance with regional geological data and previous researches. In addition, it is also supported by the findings of outcrops in the form of weathered peridotite outcrops and the presence of swamps in the manifestation area which can be seen in Figure 12.

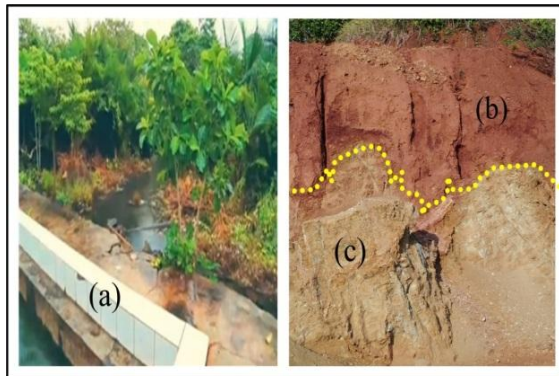


Figure 12. (a) Alluvium deposits in the form of swamps, (b) laterite soil, and (c) weathered peridotite outcrop.

Figure 10 and Figure 11 also show that in the research area there are several minor faults that pass through the peridotite and conglomerate layers. The estimated locations of these minor faults are:

1. Fault F1 is thought to be located at coordinates $4^{\circ}1'16.149''$ South Latitude and $122^{\circ}7'9.609''$ East Longitude to $4^{\circ}1'18.488''$ South Latitude and $122^{\circ}7'15.384''$ East Longitude which is ± 15 meters from the geothermal manifestation (hot springs).
2. Fault F2 is thought to be located at coordinates $4^{\circ}1'23.388''$ South Latitude and $122^{\circ}7'24.326''$ East Longitude to $4^{\circ}1'27.501''$ South Latitude and $122^{\circ}7'33.012''$ East Longitude, which is ± 28 meters from the manifestation (hot springs).
3. Fault F3 is thought to be located at coordinates $4^{\circ}1'10.041''$ South Latitude and $122^{\circ}7'10.589''$ East Longitude to $4^{\circ}1'13.041''$ South Latitude and $122^{\circ}7'14.705''$ East Longitude with a distance of ± 35 meters from the manifestation (hot springs).

4. Fault F4 is thought to be located at coordinates $4^{\circ}1'22.315''$ South Latitude and $122^{\circ}7'25.689''$ East Longitude to $4^{\circ}1'27.109''$ South Latitude and $122^{\circ}7'31.910''$ East Longitude with a distance of ± 30 meters from the manifestation (hot springs).

Regionally, the research area is influenced by the Konawehea shear fault which is trending Northwest-Southeast [28]. It is suspected that the movement of this shear fault has caused minor faults in the geothermal area of Sonai Village and its surroundings. These minor faults become the migration path for hot fluids to the surface. Meanwhile, the impermeable peridotite layer functions as bedrock in the geothermal area of Sonai Village and its surroundings.

The geothermal type of Sonai Village and its surroundings is non-volcanic geothermal, whose fluids come from surface water or meteoric water, and are controlled by fractures in the form of minor faults. The existence of a basin (Figure 7 (b)) which has a thick sedimentary layer in the form of sand and clay at the research location allows hot fluids to be distributed or infiltrated through this layer which has high permeability.

CONCLUSION

2D modeling of pseudo-gravity transformation results on residual magnetic field anomaly maps provides an overview of the subsurface layers and structures. The subsurface layers of the research area are composed of 3 formations, namely Alluvium Deposits, Alangga Formation and Ultramafic Complex. Alluvium deposits are in the form of sand with a density value of 1.5 mGal and claystone with a density value of 2.5 mGal. In the Alangga Formation, it consists of sandstone with a density value of 2.32 mGal to 2.6 mGal and conglomerate with a density value of 2.78 mGal. While in the Ultramafic Complex, there is peridotite with a density value of 2.84 mGal. This layer functions as bedrock in the geothermal area of Sonai Village and its

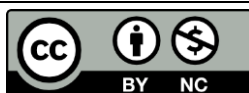
surroundings because of its impermeable nature.

The geological structures found are several minor faults. These minor faults are thought to be the migration path of hot fluids towards the surface. The two minor faults closest to the manifestation (hot springs) are located at coordinates around 4°1'16.149" South Latitude and 122°7'9.609" East Longitude which are ± 15 meters away and at coordinates around 4°1'23.388" South Latitude and 122°7'24.326" East Longitude which are ± 28 meters away from the geothermal manifestation.

REFERENCES

1. Hermawan, D., Sugianto, A., Yushantarti, A., Dahlan, Munandar, A., dan Widodo, S. (2011). Kajian Panasbumi Non Vulkanik Daerah Sulawesi Bagian Tenggara. Bandung: Pusat Sumber Daya Geologi, Kementerian ESDM.
2. Surono. (2013). Geologi Lengan Tenggara Sulawesi. Bandung: Badan Geologi, Kementerian ESDM.
3. Risdianto, D., Permana, L. A., Wibowo, A. E., Sugianto, A., & Hermawan, D. (2015). Sistem Panasbumi Non Vulkanik di Sulawesi. Bandung: Pusat Sumber Daya Mineral, Batubara dan Panas Bumi, Badan Geologi, Kementerian ESDM.
4. Brophy, P. (2011). An Introduction to Geothermal Energy. CGEC Geothermal Outreach Workshop. California: EGS Inc.
5. Gupta, H. & Roy, S. (2007). Geothermal Energy. Amsterdam: Elsevier.
6. Anonymous. (2017). Buku Potensi Panas Bumi Indonesia Jilid 2. Jakarta: Pusat Sumber Daya Mineral, Batubara dan Panas Bumi, Badan Geologi, Kementerian ESDM.
7. Baskara, M. Y. (2020). Identifikasi Sebaran Fluida Panas Daerah Panasbumi Puriala, Kabupaten Konawe Menggunakan Metode Geolistrik Resistivitas Konfigurasi Wenner-Schlumber. Skripsi. Universitas Halu Oleo.
8. Sariani, Manan, A., Bahdad & Chahyani, R. (2024). Estimation of subsurface structure using Euler Deconvolution method of magnetic data at the geothermal area of Sonai Village and its surroundings, Konawe Regency. *Jurnal Geoceleses*, **8**(2), 162–177.
9. Medhus, A. B. & Klinkby, L. (2023). Engineering Geophysics, 1st Edition. Leiden: CRC Press.
10. Telford, M. W., Geldard, L. P., Sheriff, R. E., & Keys, D.A. (1990). Applied Geophysics 2nd ed. London: Cambridge University Press.
11. Safrilia, P., Muhardi & Perdhana, R. (2024). Pemodelan 2D Struktur Geologi Bawah Permukaan di Daerah Manifestasi Panas Bumi Buaran, Kabupaten Brebes, Berdasarkan Anomali Magnetik. *JFT: Jurnal Fisika dan Terapannya*, **11**(1), 91–106.
12. Hanatha, F. D. & Hamid, H. (2024). Integrasi metode gravity dan metode geomagnetik menggunakan Dekonvolusi Euler untuk delineasi struktur pada sistem panas bumi di kawasan Candi Umbul-Telomoyo, Magelang, Jawa Tengah. *Jurnal Geosains dan Teknologi*, **7**(1), 19–28.
13. Puspita, M. B., Perwita, C. A., Maryanto, S., & Suyanto, I. (2023). Analisis Metode Magnetik pada Daerah Manifestasi Panas Bumi Karangrejo, Kabupaten Pacitan. *INSOLOGI: Jurnal Sains dan Teknologi*, **2**(5), 907–916.
14. Luthfin, A. & Jubaidah, N. A. (2023). Identification of geothermal distribution in the Banyu Biru hot water source using the magnetic method. *Indonesian Journal of Applied Physics (IJAP)*, **13**(2), 215–25.
15. Tanjung, R. U. S., Pujiastuti, D., & Putra, A. (2023). Interpretasi struktur bawah permukaan menggunakan data anomali medan magnet daerah manifestasi panas bumi Sampuraga Kabupaten Mandailing Natal. *Jurnal Fisika Unand*, **12**(4), 554–560.

16. Hidayat, H., Putra, A., & Pujiastuti, D. (2021). Identifikasi sebaran anomali magnetik pada daerah prospek panas bumi Nagari Aie Angek, Kabupaten Tanah Datar. *Jurnal Fisika Unand (JFU)*, **10**(1), 48–54.
17. Sitorus, E. & Tampubolon, T. (2018) Penentuan struktur bawah permukaan area panas bumi Tinggi Raja Kabupaten Simalungun dengan menggunakan metode magnetik. *Jurnal Einstein*, **6**(1), 26–33.
18. Simandjuntak, T. O., Surono, & Hadiwijoyo, S. (1993). Peta Geologi Lembar Kolaka Skala 1:250.000. Pusat Penelitian dan Pengembangan Geologi.
19. Zakaria, Z. & Sidarto. (2015). Aktivitas tektonik di Sulawesi dan sekitarnya sejak mesozoikum hingga kini sebagai akibat interaksi aktivitas tektonik lempeng tektonik utama di sekitarnya. *Jurnal Geologi dan Sumberdaya Mineral*, **16**(3), 115–127.
20. Surono & Hartono, U. (2013). Geologi Sulawesi. Jakarta: LIPI Press.
21. Schmidt, A. (2009). Electrical and magnetic methods in archeological prospection. *Geophysics and Landscape Archeology*, 67–81.
22. Baranov, V. (1957) A new method for interpretation of aeromagnetic maps, pseudo-gravimetric anomalies. *Geophysics*, **22**, 359–363.
23. Alamdard, K., Ansari, A. H., & Ghorbani, A. (2009). Edge detection of magnetic body using horizontal gradient of pseudogravity anomaly. *Geophysical Research*, **40**82.
24. Pancasari, A., Safani, J., & Manan, A. (2020). Interpretasi struktur bawah permukaan daerah Kota Kendari berdasarkan data anomali medan magnetik lokal. *Jurnal Rekayasa Geofisika Indonesia (JRGI)*, **2**(2), 45–53.
25. Fikar, M., Hamimu, L., Manan, A., & Suyanto, I. (2019). Pemodelan 2D data magnetik menggunakan transformasi RTP untuk pendugaan sesar di Daerah Kasihan, Pacitan, Jawa Timur. *Jurnal Rekayasa Geofisika Indonesia (JRGI)*, **2**(01), 33–42.
26. Blakely, R. J. (1995). Potensial Theory in Gravity and Magnetics Applications. Cambridge: Cambridge University Press.
27. Blakely, R. J. & Simpson, W. (1986). Approximating edge of source bodies from magnetic or gravity anomalies. *Geophysics*, **7**(51), 1.494–1.498.
28. Tamburaka, E. (2019). Resiko dan mitigasi bencana gempa tektonik di Kabupaten Konawe. *Jurnal Askara Publik*, **3**(2), 222–235.



This article uses a license
[Creative Commons Attribution
 4.0 International License](https://creativecommons.org/licenses/by-nc/4.0/)